Trtnik, G., Kavčič, F. in Turk, G. 2009. Prediction of concrete strength using ultrasonic pulse velocity and artificial neural networks. Ultrasonics 49, 1: 53–60.
DOI: 10.1016/j.ultras.2008.05.001.

Prediction of concrete strength using ultrasonic pulse velocity and artificial neural networks

Gregor Trtnik[a,b] , Franci Kavčič[b], Goran Turk[a,*]

[a]University of Ljubljana, Faculty of Civil and Geodetic Engineering
Jamova 2, SI-1115 Ljubljana, Slovenia
[b]IGMAT d.d., Building Materials Institute, Polje 351c, Ljubljana, Slovenia

Abstract

Ultrasonic pulse velocity technique is one of the most popular non-destructive techniques used in the assessment of concrete properties. However, it is very difficult to accurately evaluate the concrete compressive strength with this method since the ultrasonic pulse velocity values are affected by a number of factors, which do not necessarily influence the concrete compressive strength in the same way or to the same extent. This paper deals with the analysis of such factors on the velocity-strength relationship. The relationship between ultrasonic pulse velocity, static and dynamic Young's modulus and shear modulus was also analyzed. The influence of aggregate, initial concrete temperature, type of cement, environmental temperature, and w/c ratio was determined by our own experiments. Based on the experimental results, a numerical model was established within the Matlab programming environment. The multi-layer feed-forward neural network was used for this purpose. The paper demonstrates that artificial neural networks can be successfully used in modelling the velocity-strength relationship. This model enables us to easily and reliably estimate the compressive strength of concrete by using only the ultrasonic pulse velocity value and some mix parameters of concrete.

Keywords: Ultrasonic pulse velocity; Young concrete; Compressive strength; Mix parameters; Artificial neural network

* Corresponding author. Phone: +386 1 4768 614; fax: +386 1 4768 629.
E-mail address: gturk@fgg.uni-lj.si

Introduction

Numerous attempts to use ultrasonic pulse velocity V_p [km/s] as a measure of the compressive strength of concrete S [MPa] has been made, due to the obvious advantages of non-destructive testing methods. The evaluation of concrete compressive strength is usually based on empirical relations between strength and non-destructive parameters. Manufacturers usually give such relationships for their own testing systems, which are not suitable for every kind of concrete. Therefore, they need to be calibrated for different mixtures. The conventional approach to derive such mathematical relationships by means of regression analysis has not been very successful [1]. Numerous data and the correlation relationships between strength and V_p of concrete have been proposed and presented. The most popular such formula is

$$S = a \ \exp(b\, V_p), \tag{1}$$

where a and b are empirical parameters determined by the least squares method. Table 1 presents some relationships between concrete compressive strength S and the ultrasonic pulse velocity of longitudinal waves V_p, together with the coefficients of determination R^2.

Table 1

It can be seen from Table 1, that the coefficients of determination are low because the concrete composition was not taken into account. It is known that many factors that influence concrete strength also influence pulse velocity, though not necessarily in the same way or to the same extent [1]. The presence of aggregate affects the relationship between pulse velocity and the compressive strength of concrete. At the same strength level, concrete with the highest aggregate content will probably have the highest pulse velocity [6]. Cement type influences pulse velocity and on the other hand, it influences the compressive strength of concrete, too. It was found that a higher water content affects the propagation velocity

approximately in proportion to the change of the water content in concrete [7]. The results of experiments, performed by Bernardo [8], also show that a higher water content leads to a higher pulse velocity through concrete. It was also found that a higher water content leads to a lower compressive strength of concrete [9]. Such dissimilarities create ambiguity in the interpretation of the ultrasonic results. The age of concrete is also an important factor. The pulse velocity after one day is about 3.8 km/s and after three years it is about 5.2 km/s. That is, the velocity increases by about 40% after three years. The increase in the compressive strength during the same period is much higher, more than 500% [1].

The first objective of this study was to identify the effect of concrete mix parameters, including the aggregate gradation, type of aggregate, type of cement, and water-cement ratio, on the relationship between ultrasonic pulse velocity, V_p, and compressive strength, S, static, Es, and dynamic, Ed, Young's modulus and shear modulus, G, of young concrete. Within this study, secant static Young's modulus were used. The influence of the concrete's initial temperature, T_{init}, and environmental temperature, T_{env}, on these relationships was also studied. The second objective of this study was to establish a numerical model to evaluate the concrete compressive strength, static Young's modulus, dynamic Young's modulus, and shear modulus, as a function of the ultrasonic pulse velocity in concrete and some basic characteristics of concrete mix. The multi-layer feed-forward neural network was used for this purpose.

Experimental program

To achieve the objectives of this study, a portable ultrasonic tester "Controls, Mod. 58-E0046", was used to evaluate ultrasound wave velocity into concrete specimens. The transducers used were 50 mm in diameter, and had maximum resonant frequencies of 54kHz. Resonant frequency method, described in [10], was adopted to determine the dynamic Young's modulus and shear modulus of concrete. Three types of aggregates were used within

this study. The first type of aggregate was limestone crushed aggregate, the second was limestone aggregate with rounded grains and the third type was crushed quarcit carbonate aggregate. Some properties of used aggregate, as measured in our laboratory, are summarized in Table 2, while the aggregate gradations are shown in Fig. 1. In order to check the influence of cement type, four types of cements were used, namely CEM II/A-S, 42.5R, CEM I, 52.5R, CEM I, 42.5N and CEM I, 42.5N SR.

Table 2

Several experiments were performed at the IGMAT d.d., Building Materials Institute, Ljubljana, Slovenia. Experimental work was, at the first stage, divided into two parts.

Part 1: Influence of the aggregate on the V_p - S relationship

The focus of part 1 was to capture the influence of the amount of aggregate (AA), type of aggregate (TA), nominal maximum aggregate size (MNS) and shape of aggregate (SA) on the V_p - *S*, V_p - *Es*, V_p - *Ed* and V_p - *G* relationships. 16 concrete mixtures were prepared for this purpose. The amount of limestone crushed aggregate in the reference mixture REF was 1804 kg/m^3 and the nominal maximum aggregate size was 16 mm (see Table 3).

Initial temperature of all concrete mixtures from this part was 22°C. Table 4 presents the differences between reference mixture REF and other mixtures from this part.

Table 3

Table 4

The aggregate gradations are shown in Fig. 1 and were the same for all mixtures as in the case of REF mixture, except for mixtures MNS/2, MNS/3 and MNS/4.

Fig. 1.

Part 2: Influence of the T_{init}, T_{env}, type of cement, and w/c ratio on the V_p - S relationship

The focus of part 2 was to capture the influence of the initial concrete temperature, environmental temperature, type of cement, and w/c ratio on the $V_p - S$ relationship. Nine concrete mixtures were prepared for this purpose. Table 5 shows the differences between reference mixture and other mixtures from this part. The aggregate gradation and type of aggregate were the same for all mixtures from part 2.

Table 5

Ten cubic specimens (15 cm) and three prismatic specimens (10/10/40 cm) were made for each mixture in order to obtain *S* (cubic specimens) and *Es*, *Ed* and *G* values (prismatic specimens). Immediately after mixing, the specimens were covered with plastic bags to prevent excessive water evaporation.

Measurements were performed according to the valid standards. The specimens were stored at a temperature of 20±2°C (part 1) and a relative humidity of ≥ 65%. Concrete specimens were tested in the laboratory for V_p, *S*, *Es*, *Ed* and *G* after 1, 2, 3 and 7 days. The direct transmission technique was used to determine the V_p in concrete, because this arrangement was considered to be the most satisfactory and reliable method, since the longitudinal pulses leaving the transmitter are propagated in the direction normal to the transducer face. The maximum energy of the pulse is transmitted and received using this arrangement. In order to

ensure uniform and constant pressure between transducers and concrete surfaces, the transducers were pressed by hand to apply about 10 N of constant force. Petroleum jelly was used as a couplant between the transducer and concrete surface in order to ensure full contact and to eliminate the air pocket between the transducers and the test medium. Repeated readings at a particular location were taken and a minimum value of transit time was taken as the experimental result.

Experimental results

All data

Fig. 2 shows a relationship between compressive strength S of concrete specimen and corresponding V_p for all concrete specimens. It can be seen form this Fig. that the V_p - S relationship is quite low. The best fit-curve representing this relationship is given as

$$S = 0.0854 \ \exp(1.2882 \ V_p) \tag{2}$$

Coefficient of correlation between actual compressive strengths S and compressive strengths S_{RM}, determined by proposed regression model was $R^2 = 0.6444$. σ value was found to be 7.2609 MPa and was determined according to formula

$$\sigma = \sqrt{\frac{1}{n-2}\sum_{i=1}^{n} \varepsilon_i^{\,2}} \tag{3}$$

where n is the number of all data and ε_i is the difference, determined according to the formula

$$\varepsilon_i = S - S_{RM} \,. \tag{4}$$

The reason for this low V_p - S relationship is that the concrete mixing parameters were not taken into account. As expected, the relationships between V_p and E_{stat}, E_{dyn} and G were found to be more accurate, which can be seen from Fig. 3. The variances were found to be much

lower in the case of *Es*, *Ed* and *G*. Table 6 presents both R^2 and σ values for these relationships.

Fig. 2.

Fig. 3.

Table 6.

It can be seen from Fig. 2, Fig. 3, and Table 6, that *Es*, *Ed* and *G* values can be reliably modelled by a function of V_p only, whereas *S* depends on some other parameters.

Part 1: Influence of the aggregate on the V_p - S relationship

Fig. 4 shows a relationship between the compressive strength, *S*, of a concrete specimen and the corresponding V_p for all concrete specimens from part 1. The best fit-curve representing this relationship is given as

$$S = 0.3216 \exp(0.9895\, V_p) \quad (5)$$

The correlation coefficient between *S* and S_{RM} was $R^2 = 0.5132$ and σ value was 6.5187 MPa (see Table 7). That means that the aggregate affected the V_p - *S* relationship to a high degree. Therefore, the influence of the aggregate on the V_p - *S* relationship had to be studied in detail.

Table 7.

Fig. 4.

Figure 5 clearly shows the influence of amount of aggregate, type of aggregate, nominal maximum aggregate size, and shape of aggregate, on the V_p - S relationship. In Fig. 5a, influence of the amount of aggregate in concrete is shown for mixtures with w/c ratio 0.54. It can be clearly seen, that the amount of aggregate is a very important factor that affects the V_p - S relationship. In order to verify this hypothesis, 6 supplementary mixtures with different w/c ratios, labelled AA040/1, AA040/2, AA040/3, AA065/1, AA065/2 and AA065/3 (see Table 4) were prepared. At the same strength level, mixtures with the highest (AA040/2, AA054/2, AA065/2) and the lowest (AA040/3, AA054/3, AA065/3) aggregate content have the highest and the lowest pulse velocity, respectively. That means that the amount of aggregate in concrete does not affect the V_p and S to the same degree. Moreover, in some cases, the higher aggregate content can cause an increase in the V_p and decrease in S. This phenomenon can be clearly observed from Fig. 6a, where influence of amount of aggregate on V_p and S is shown for mixtures with w/c ratio 0.54. Interestingly, w/c ratio did not play an important part, when the influence of the amount of aggregate on the V_p - S relationship was studied. This can be clearly observed from Fig. 6b, where the influence of the amount of aggregate on V_p - S relationship for mixtures with different w/c ratios is shown. Mixtures AA040/1, REF and AA065/1 together are labelled as group GAA1, mixtures AA040/2, AA054/2 and AA065/2 are labelled as GAA2 and mixtures AA040/3, AA054/3 and AA065/3 are labelled as GAA3. The correlation coefficients between S and S_{RM} for groups GAA1, GAA2 and GAA3 are quite high and are shown in Table 7. Of course, both S and V_p values were higher in the case of lower w/c ratio. The increase in V_p with the increase of aggregate content can be also

observed from Eq. 6 [11]. If the concrete is considered as a two-phase medium consisting of a cement paste phase and an aggregate phase, the V_p of concrete can be calculated as

$$\frac{1}{V_p} = \frac{V_{cem}}{v_p} + \frac{V_{agg}}{v_{agg}} \tag{6}$$

where V_{cem} and V_{agg} are the volume percentages of cement paste and aggregate in the concrete, respectively and v_p and v_{agg} are the longitudinal ultrasonic velocities in cement paste and aggregate, respectively. Berriman et al. established a strong positive linear correlation between aggregate content and speed of sound [12].

Fig. 5b shows the influence of the type of aggregate on the V_p - S relationship. It is evident that the type of aggregate affects this relationship. Mixtures TA2/1, TA2/2 and TA2/3, which were prepared with crushed quarcit carbonate aggregate, had lower compressive strength and lower ultrasonic pulse velocity. The reason for this lower V_p is relatively low value of V_p through this type of aggregate (see Table 2). Even though mixtures with highest (TA2/2) and lowest (TA2/3) aggregate content have the highest and the lowest pulse velocity at the same strength level also for this type of aggregate, this difference was not as significant as in the case of limestone aggregate. The influence of aggregate type on the V_p - S relationship can be also seen from Table 7, where the correlation coefficients between S and S_{RM} for groups GTA1 (mixtures REF and TA2/1 together), GTA2 (AA054/2, TA2/2) and GTA3 (AA054/3, TA2/3) are shown. Relatively low values of R^2 confirm this hypothesis.

Fig. 5c shows the influence of the nominal maximum aggregate size on the V_p - S relationship for mixtures with w/c ratio 0.54. At the same V_p level, mixtures with the lowest (*MNS/4*) and the highest (*MNS4/2*) nominal aggregate size have the highest and the lowest compressive strength S, respectively.

The influence of the shape of aggregate is shown in Fig. 5d for mixtures with w/c ratio 0.54. At the same V_p level, a mixture with the rounded aggregate grains (SA/2) has lower

compressive strength S than mixture with crushed aggregate shape (REF). This can be explained by the fact that the contact between aggregate grains and cement paste is weaker in the case of rounded aggregate grains, leading to a reduction in the concrete strength [13].

Fig. 5.

Fig. 6.

Part 2: Influence of the T_{init}, T_{env}, cement type, and w/c ratio on the V_p - S relationship

Fig. 7 shows the relationship between compressive strength S and corresponding V_p for all concrete specimens from part 2. The best fit-curve representing this relationship is given by

$$S = 0.0312 \ \exp(1.4896 \ V_p) \tag{7}$$

and the R^2 and σ values are 0.9523 and 3.6900 MPa, respectively (see Table 7). The proposed regression model described the relationship between V_p and S quite well in this case, so it can be concluded, that the influences of T_{ini}, T_{env}, type of cement, and w/c ratio on the V_p - S relationship within this range of values were not very important. As expected, both S and V_p values were the highest and the lowest in the case when cement CEM I, 52.5R and CEM I, 42.5 N SR were used, respectively. The fact that cement type does not appear to have a significant effect on V_p - S relationship can be also seen from Table 7, where relatively high value of correlation coefficient between S and S_{RM} for all mixtures with different cement type together (group GTC) can be found.

Fig. 7.

Numerical model for determination of compressive strength of young concrete with ultrasonic pulse velocity method

Based on the experimental results, presented in the previous section, a numerical model was established in order to evaluate the concrete's compressive strength by the determination of the ultrasonic pulse velocity in arbitrary concrete. The artificial neural network (ANN) approach was used for this purpose. ANNs are increasingly applied to solve various civil engineering problems. Recently, there have been reports on the use of ANN in the modelling of concrete compressive strength [14,15,16] but lately, some applications of ANNs to determine concrete compressive strength based on non-destructive tests have also been presented. Hola et al. [17,18] presented a neural network approach to determine concrete compressive strength, based on several non-destructive tests. It has been repeatedly pointed out that the determination of concrete compressive strength would be more accurate, and thus more reliable, if it was based on several parameters determined by different non-destructive techniques. The use of V_p alone seemed to be over-optimistic. Kewalramani [19] reported an ANN model to predict the compressive strength of concrete using ultrasonic pulse velocity alone, based on weight and V_p for two different concrete mixtures.

In this study, an ANN approach for prediction of the compressive strength of arbitrary young concrete is presented, based on the concrete mix parameters and V_p.

Artificial neural networks

ANNs are algorithms simulating the functioning of biological neurons. The motivation for the development of neural network technology stemmed from the desire to develop an artificial system that could perform intelligent tasks similar to those performed by the natural brain. ANNs represent simplified methods of a human brain and may be used to solve problems that conventional methods with traditional computations find difficult to solve.

The ANN is a network of simple units (neurons) which operate locally. A typical multi-layer feed-forward neural network, which was used in this study, has three or more layers: the input layer, one or more hidden layers, and the output layer.

The set of input and output values is termed an input-output pair. All such pairs are often divided into two sets. The first one is termed as the learning (training) set which is used to determine the connection weights and thresholds. When the learning procedure ends, meaning that the neural networks perform adequately for all input-output pairs in the learning set, the neural network is assessed on the testing set of data. Detailed description of the theoretical background of ANNs is presented elsewhere [14, 15, 16, 17, 18, 19].

ANN-based prediction numerical model

The results of the experimental work, described in previous sections, showed that the initial temperature of fresh concrete, the environmental temperature, type of cement and the w/c ratio, had no significant effect on the V_p - S relationship within presented ranges of values and that the Es, Ed and G values can be reliably and accurately modelled by a function of V_p only. Therefore, the input layer of proposed ANN was modelled with five input neurons corresponding to the amount of aggregate (AA), nominal maximum aggregate size (MNS), aggregate type (TA), shape of aggregate (SA), and V_p, whereas the output layer was represented by one output neuron corresponding to the compressive strength S. Different sizes of learning and testing sets were tried; however, the results did not differ considerably. Finally, 70% of randomly selected pairs were used for learning and the remaining 30% were used as testing pairs.

Many calculations with different geometries of ANNs were carried out. On the basis of the results, the final solution was calculated with the geometry 5-30-30-1, i.e. there were two hidden layers, each of them including 30 neurons. The structure of proposed ANN is shown in

Fig. 8. The efficiency of the learning procedure was very good. The coefficient of correlation between actual and calculated values belonging to the testing set was $R^2 = 0.9954$.

When all the weights $w_{ij,k}$ were determined, a numerical program was established within the Matlab programming environment to evaluate the concrete compressive strength S with the determination of the V_p in arbitrary concrete.

Some specimens, which were not included in learning set, were tested with proposed neural network model. These were specimens from mixtures AA040/2, AA040/3, AA065/2 and AA065/3. 36 additional cubic specimens were also prepared in order to validate proposed neural network model. Characteristics of these extra specimens are shown in Table 8:

Table 8.

These specimens were tested for V_p and S after randomly chosen days (max. 7 days).

Fig. 8.

Results and discussion

The efficiency of proposed numerical model can be seen from Fig. 9. Fig 9a shows the relationship between actual compressive strength S and compressive strength S_{RM}, determined from nonlinear regression model (2) for all concrete specimens, including additionally prepared concrete specimens (see Table 8). The coefficient of correlation was $R^2 = 0.62$ in this case, which is in good agreement with the coefficients of correlation, proposed by other researchers (see Table 1). Fig 9b shows the relationship between S and compressive strength S_{ANN} for the same concrete specimens, determined from proposed numerical model. It clearly depicts that experimentally evaluated values, S, are in strong coherence with the values S_{ANN},

predicted through proposed ANN numerical model. This is evidenced by the fact that the lozenges lie close to the centre line, corresponding to the ideal mapping, as well as by the relatively high correlation coefficient value R^2 = 0.84. The nearer the points gather at the diagonal, the better are the results.

The efficiency of the proposed model is even more clearly observed from Fig. 9c and Fig. 9d, where the results of concrete specimens from part 1 only are shown, including additionally prepared concrete specimens, where the influence of the important factors data, established in this study, were taken into account. The difference between R^2 values between S - S_{RM} and S - S_{ANN} is even greater in this case.

Fig. 9e and 9f show the correlation between S - S_{RM} (model 2) and S - S_{ANN} values for additionally prepared concrete specimens only (see Table 8), which were not used in ANN learning procedure. The significant difference between R^2 values between S - S_{RM} and S - S_{ANN} can be clearly observed.

Therefore, this result clearly indicates, that over-fitting hasn't occurred during the learning procedure, since the correlation is relatively high (R^2 = 0.80) also in the case of new data which was not used in training.

Fig. 9.

Conclusions

Numerous attempts to use ultrasonic pulse velocity as a measure of compressive strength of concrete has been made on the basis of conventional computational techniques like multiple regression analysis. Most of these studies did not consider, or failed to evaluate the effect of concrete mix parameters on the ultrasonic pulse velocity - compressive strength relationship. The present work utilizes artificial neural network to predict compressive strength of young

concrete based on ultrasonic pulse velocity and some concrete mix parameters. The influence of the amount of aggregate, nominal maximum aggregate size, type of aggregate, shape of aggregate, type of cement, initial concrete temperature, environmental temperature, and w/c ratio on the strength - velocity relationship, was studied, based on our own experiments. It was shown that the influence of aggregate is very important and cannot be neglected for accurate prediction of compressive strength of concrete based on ultrasonic pulse velocity. The prediction of concrete compressive strength with the proposed numerical model, which was established within Matlab programming environment, showed a good degree of coherency with experimentally estimated compressive strength. Thus, the present study shows that the determination of concrete compressive strength, based on ultrasonic pulse velocity alone, can be predicted very accurately if properly considered. With this model, one can easily and accurately determine the compressive strength of arbitrary concrete only by knowing the ultrasonic pulse velocity and some concrete mix characteristics. It does not need a specific equation that differs from traditional prediction models. Also, this model can continuously re-train new data, so that it can conveniently adapt to new data in order to expand the range of suitability of ANN. This becomes available with new experiments.

Acknowledgements

The work of G. Trtnik was financially supported by the Ministry of Education, Science and Sport of the Republic of Slovenia under contract 3211-05-000556. The support is gratefully acknowledged.

References

1. S. Popovics, Analysis of the concrete strength versus ultrasonic pulse velocity relationship, American Society for Nondestructive Testing, 2007, http://www.asnt.org/publications/materialseval/basics/feb01basics/feb01basics.htm.

2. P. Turgut, Evaluation of the Ultrasonic Pulse Velocity Data Coming on the Field, 4th International Conference on NDE in Relation to Structural Integrity for Nuclear and Pressurised Components, London, 2004.
3. I. H. Nash't, S. H. A'bour, A. A. Sadoon, Finding an Unfied Relationship between Crushing Strength of Concrete and Non-destructive Tests, Middle East Nondestructive Testing Conference & Exhibition, Bahrain, 2005.
4. G. F. Kheder, A two stage procedure for assessment of in situ concrete strength using combined non-destructive testing, Materials and Structures 32 (1999) 410-417.
5. L. M. del Rio, A. Jimenez, F. Lopez, F. J. Rosa, M. M Rufo, J. M. Paniagua, Characterization and hardening of concrete with ultrasonic testing, Ultrasonics 42 (2004), 527-530.
6. G. I. Crawford, Guide to Nondestructive Testing of Concrete, Technical Report No. FHWA-SA-97-105, U.S. Department of Transportation, September, 1997.
7. E. Ohdaira, N. Masuzawa, Water content and its effect on ultrasound propagation in concrete – the possibility of NDE, Ultrasonics 38 (2000) 546-552.
8. M. Bernardo, Application of Through Transmission Ultrasonics to Determine the Moisture Content in Concrete, B. Sc. Thesis, Brisbane, October, 2003.
9. G. Li, The effect of moisture content on the tensile strength properties of concrete, Master Thesis, Florida, 2004.
10. Standard ASTM E 1876-99, Standard Test Method for Dynamic Young's Modulus, Shear Modulus, and Poisson's Ratio by Impulse Excitation of Vibration, July, 1999.
11. G. Ye, Experimental study and numerical simulation of the development of microstructure and permeability of cementitious materials, PhD Theses, Delft, 2003.

12. J. Berriman, P. Purnell, D. A. Hutchins, A. Neild, Humidity and aggregate content correction factors for air-coupled ultrasonic evaluation of concrete, Ultrasonics 43 (2005) 211-217.
13. P. K. Mehta, Concrete structure, properties and materials. NJ: Prentice-Hall, 1986.
14. N. Hong-Guang, W. Ji-Zong, Prediction of compressive strength of concrete by neural networks, Cement and Concrete Research 30 (2000) 1245-1250.
15. S. Ali, M. Serra, Concrete strength prediction by means of neural network, Construction and Building Materials 11 (1997) 93-98.
16. S. C. Lee, Prediction of concrete strength using artificial neural networks, Engineering Structures 25 (2003) 849-857.
17. J. Hola, K. Schabowicz, Application of artificial neural networks to determine concrete compressive strength based on non-destructive tests, Journal of Civil Engineering and Management 11 (2005) 23-32.
18. J. Hola, K. Schabowicz, New technique of nondestructive assessment of concrete strength using artificial intelligence, NDT&E International 38 (2005) 251-259.
19. M. A. Kewalramani, R. Gupta, Concrete compressive strength prediction using ultrasonic pulse velocity through artificial neural networks, Automation in Construction 15 (2006) 374-379.

Table 1: Relationships between concrete compressive strength and ultrasonic pulse velocity.

Equation	R^2	Ref.
$S = 1.146 \exp(0.77\ V_p)$	0.80	[2]
$S = 1.19 \exp(0.715\ V_p)$	0.59	[3]
$S = 8.4*10^{-9}(V_p*10^3)^{2.5921}$	0.42	[4]*
$S = 1.2*10^{-5}(V_p*10^3)^{1.7447}$	0.41	[4]**
$S = \exp[(-3.3\pm1.8)+(0.0014\pm0.0004)\ (V_p*10^3)]$	0.48	[5]

* for wet concrete, ** for dry concrete

Table 2: Physical properties of aggregate used in concrete mixtures

aggregate type	physical properties	magnitude of physical properties
crushed limestone	specific gravity	2.71
	V_p [km/s]	4.8 - 5.2
rounded limestone	specific gravity	2.71
	V_p [km/s]	4.8 - 5.2
crushed quarcit carbonate	specific gravity	2.55
	V_p [km/s]	2.8 - 3.7

Table 3: Characteristics of reference mixture REF

cement	type	CEM II/A-S, 42.5 R
	amount [kg/m^3]	370
aggregate	shape	Crushed limestone
	amount [kg/m^3]	1804
	sand [%]	7
	0/4 mm [%]	44
	4/8 mm [%]	20
	8/16 mm [%]	29
	16/32 mm [%]	-
water	amount [kg/m^3]	204
additives	-	
w/c ratio	0.54	
T_{init} [°C]	22	
T_{env} [°C]	20±2	

Table 4: Differences with respect to the reference mixture - part 1

mixture name	amount of aggregate [kg/m^3]	type of aggregate	max. grain size [mm]	shape of aggregate	w/c ratio
AA054/2	2131	-	-	-	-
AA054/3	1500	-	-	-	-
MNS/2	-	-	32	-	-
MNS/3	-	-	8	-	-
MNS/4	-	-	4	-	-
SA/2	-	-	-	rounded	-
AA040/1	-	-	-	-	0.4
AA040/2	2131	-	-	-	0.4
AA040/3	1500	-	-	-	0.4
AA065/1	-	-	-	-	0.65
AA065/2	2131	-	-	-	0.65
AA065/3	1500	-	-	-	0.65
TA2/1	-	quarcit carbonate	-	-	-
TA2/2	2131	quarcit carbonate	-	-	-
TA2/3	1500	quarcit carbonate	-	-	-

Table 5: Differences according to the reference mixture - part 2

mixture name	T_{init} [°C]	T_{env} [°C]	w/c ratio	type of cement
T2	8	−1	-	-
T3	8	−1	0.45	-
T4	8	−1	0.50	-
T5	12	10	0.45	-
T6	8	10	0.45	-
TC2	-	-	-	CEM I, 42.5N
TC3	-	-	-	CEM I, 52.5R
TC4	-	-	-	CEM I, 42.5N SR

Table 6. Statistical analysis of the regression models, all data

parameter	R^2	σ [Mpa]	regression model
S	0.64	7.26	$S = 0.0854 \exp(1.2882\ V_p)$
Es	0.89	1.31	$Es = 12.435\ V_p - 25.20$
Ed	0.92	1.07	$Ed = 11.796\ V_p - 18.31$
G	0.93	0.39	$G = 4.84\ V_p - 7.94$

Table 7. Statistical analysis of the regression models for individual V_p - S relationships

label	R^2	σ	MRM
part 1	0.51	6.52	$S = 0.3216 \exp(0.9895\ V_p)$
part 2	0.95	3.69	$S = 0.0312 \exp(1.4896\ V_p)$
REF	0.92	2.01	$S = 0.0607 \exp(1.3620\ V_p)$
AA054/2	0.97	1.37	$S = 0.0673 \exp(1.2390\ V_p)$
AA054/3	0.99	0.86	$S = 0.1017 \exp(1.3750\ V_p)$
MNS/2	0.87	3.00	$S = 0.0167 \exp(1.6380\ V_p)$
MNS/3	0.96	1.13	$S = 0.0184 \exp(1.6920\ V_p)$
MNS/4	0.98	0.66	$S = 0.0833 \exp(1.4230\ V_p)$
SA/2	0.99	0.96	$S = 0.1448 \exp(1.1006\ V_p)$
AA040/1	0.94	1.77	$S = 0.0157 \exp(1.6735\ V_p)$
AA040/2	0.90	2.62	$S = 0.0043 \exp(1.8238\ V_p)$
AA040/3	0.95	1.86	$S = 0.0150 \exp(1.7680\ V_p)$
AA065/1	0.88	2.51	$S = 0.0297 \exp(1.5572\ V_p)$
AA065/2	0.94	1.40	$S = 0.0161 \exp(1.6530\ V_p)$
AA065/3	0.98	1.00	$S = 0.0215 \exp(1.7487\ V_p)$
TA2/1	0.93	2.03	$S = 0.0002 \exp(3.0036\ V_p)$
TA2/2	0.93	1.44	$S = 0.0001 \exp(3.1846\ V_p)$
TA2/3	0.90	2.31	$S = 0.0003 \exp(2.9494\ V_p)$
TC2	0.97	1.44	$S = 0.0255 \exp(1.5692\ V_p)$
TC3	0.89	2.78	$S = 0.0193 \exp(1.6574\ V_p)$
TC4	0.99	0.94	$S = 0.0246 \exp(1.5999\ V_p)$
GAA1	0.96	2.23	$S = 0.0459 \exp(1.4387\ V_p)$
GAA2	0.91	3.29	$S = 0.1028 \exp(1.1744\ V_p)$
GAA3	0.94	2.92	$S = 0.0764 \exp(1.4167\ V_p)$
GTA1	0.74	3.50	$S = 0.1575 \exp(1.1568\ V_p)$
GTA2	0.81	3.03	$S = 0.2928 \exp(0.9303\ V_p)$
GTA3	0.82	3.21	$S = 0.0619 \exp(1.5064\ V_p)$
GTC	0.93	2.67	$S = 0.0256 \exp(1.5794\ V_p)$

Table 8. Basic characteristics of additionally prepared cubic specimens

number of specimens	amount of agg. [kg/m^3]	type of aggregate	max. grain size [mm]	shape of aggregate	w/c ratio	type of cement
1-6	1750	limestone	32	crushed	0.45	CEM I, 42.5N
7-12	1530	limestone	8	crushed	0.45	CEM I, 42.5N
13-18	1804	quarc. carb.	4	crushed	0.6	CEM I, 52.5R
19-24	2000	quarc. carb.	32	rounded	0.6	CEMI I,42.5N
25-30	1530	limestone	4	rounded	0.5	CEM II/A-S, 42.5R
31-36	2000	limestone	8	crushed	0.5	CEM I,42.5 N SR

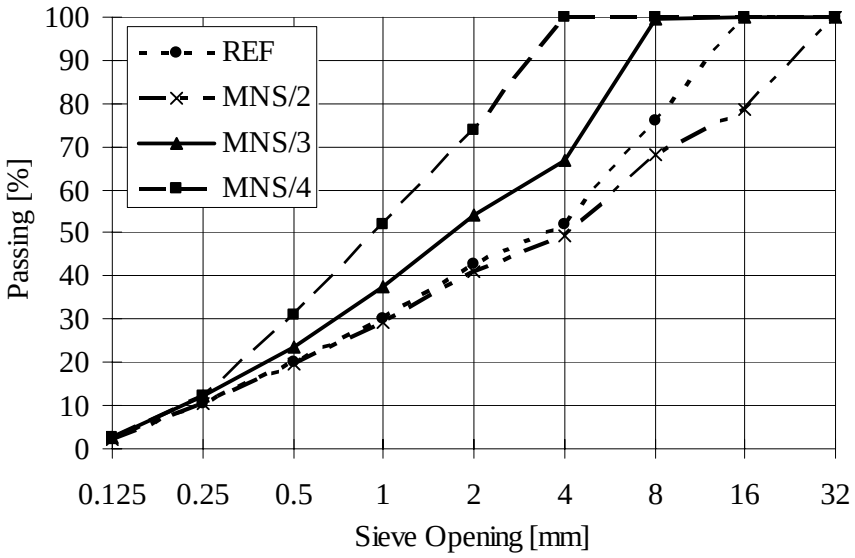

Fig. 1. Gradations of aggregate used in preparing concrete specimens

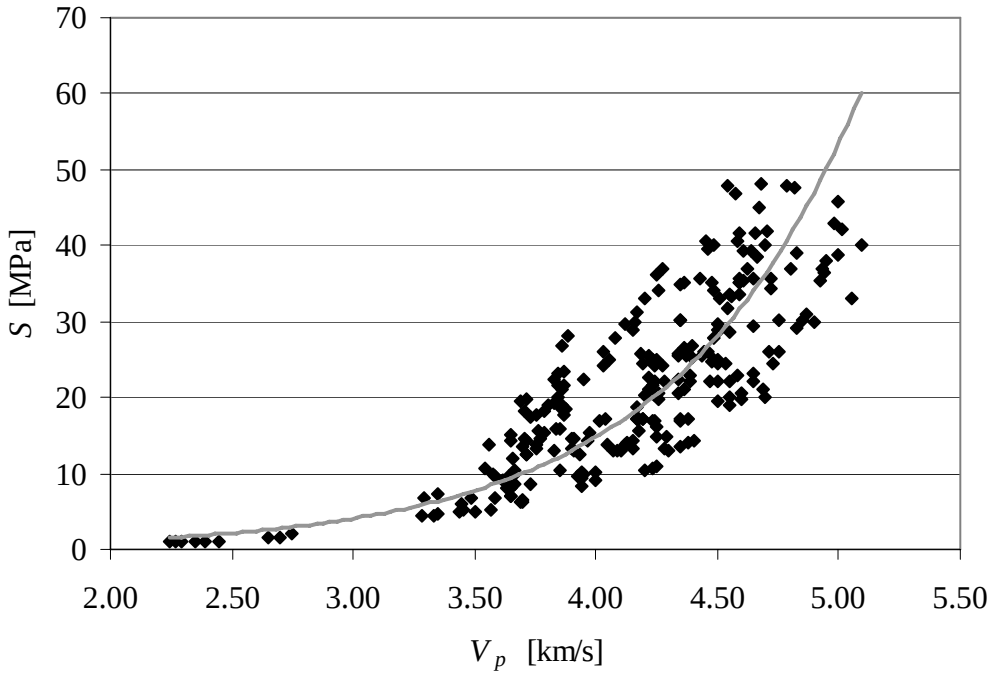

Fig. 2. Relationship between V_p and S for all data

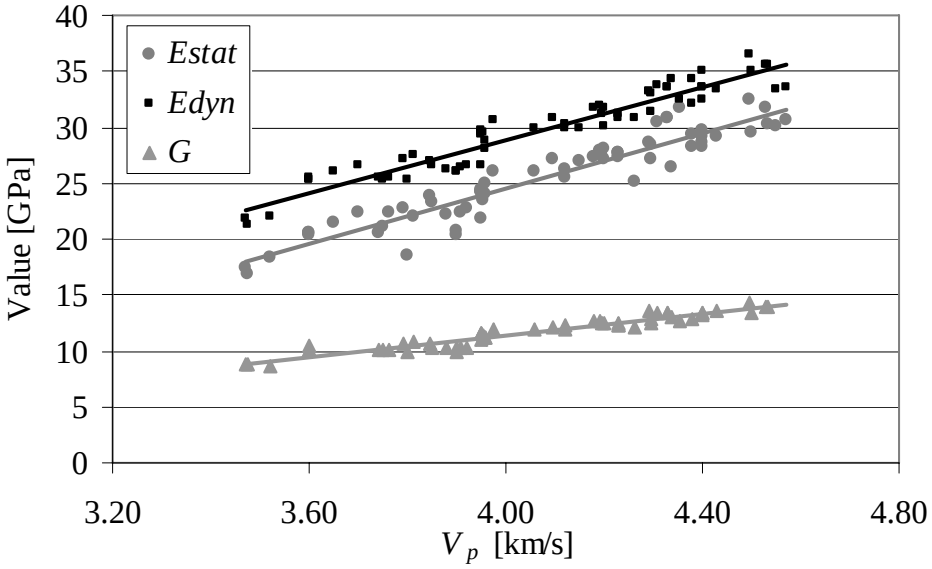

Fig. 3. Relationships between V_p and *Es*, *Ed* and *G* for all data

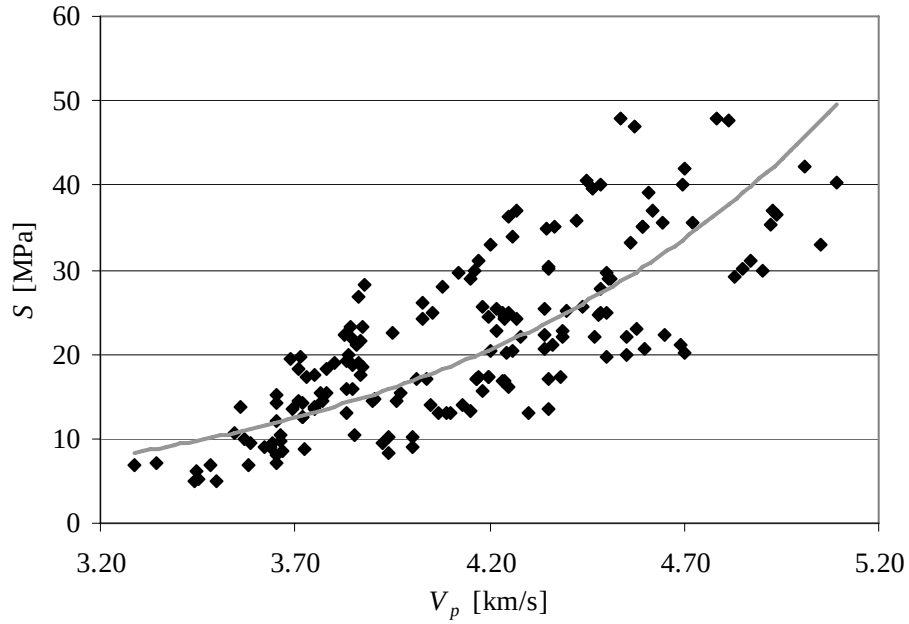

Fig. 4. Relationship between V_p and S, part 1

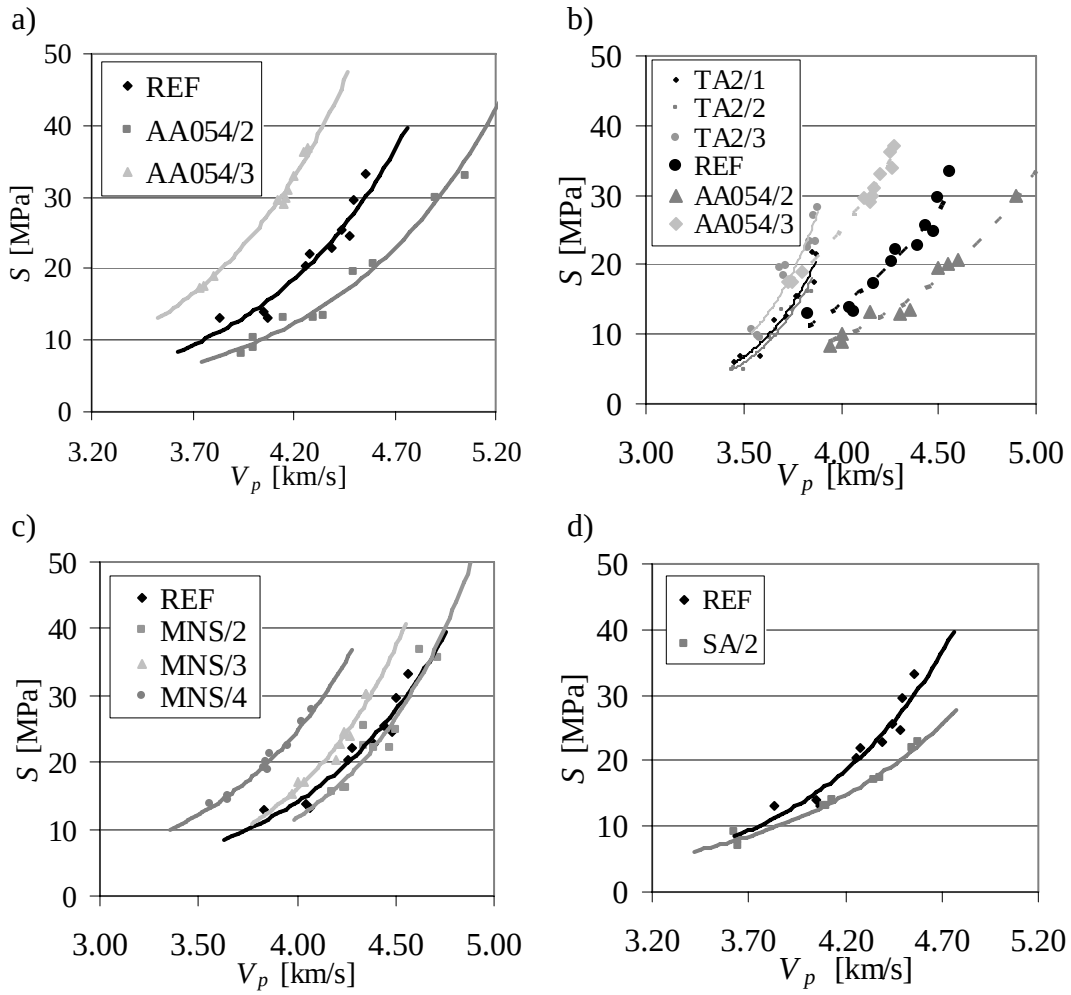

Fig. 5. Influence of the aggregate on the V_p - S relationship. a) Influence of amount of aggregate, b) Influence of aggregate type, c) Influence of nominal maximum aggregate size, d) Influence of shape of aggregate.

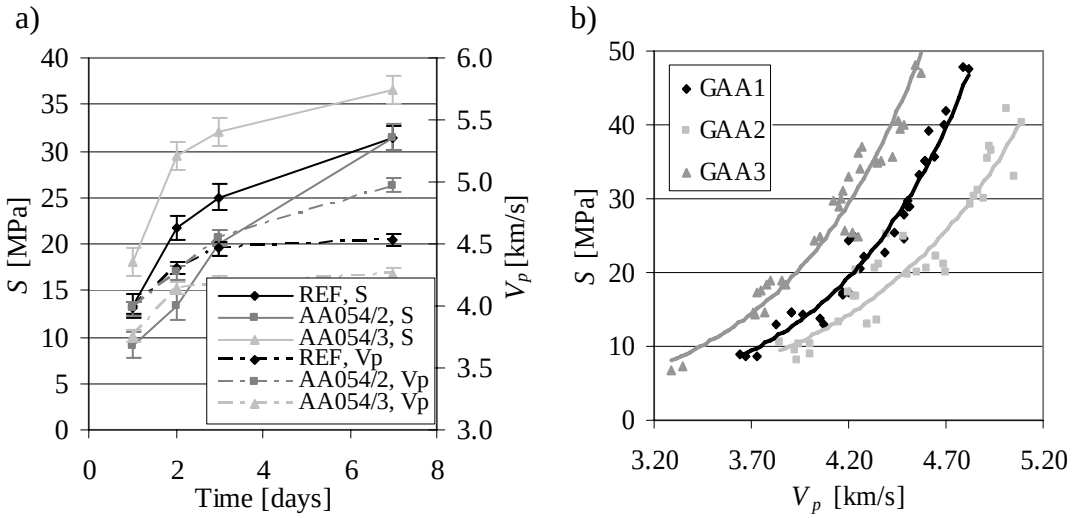

Fig. 6. Influence of the aggregate on the V_p - S relationship. a) Influence of amount of aggregate on S and V_p, mixtures with w/c = 0.54, b) Influence of amount of aggregate on V_p – S relationship for mixtures with different w/c ratio.

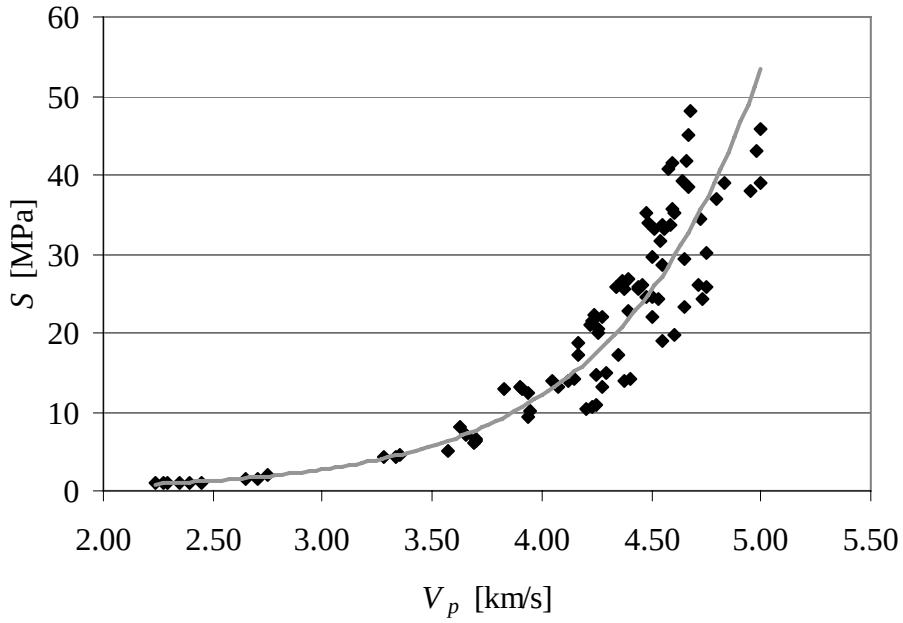

Fig. 7. Relationship between V_p and S, part 2

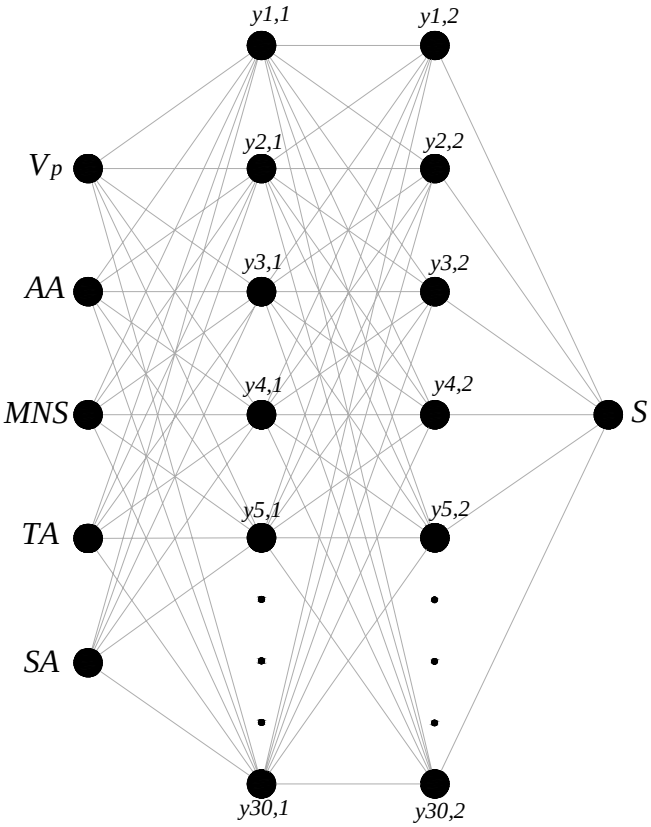

Fig. 8. Structure of the proposed 5-30-30-1 ANN

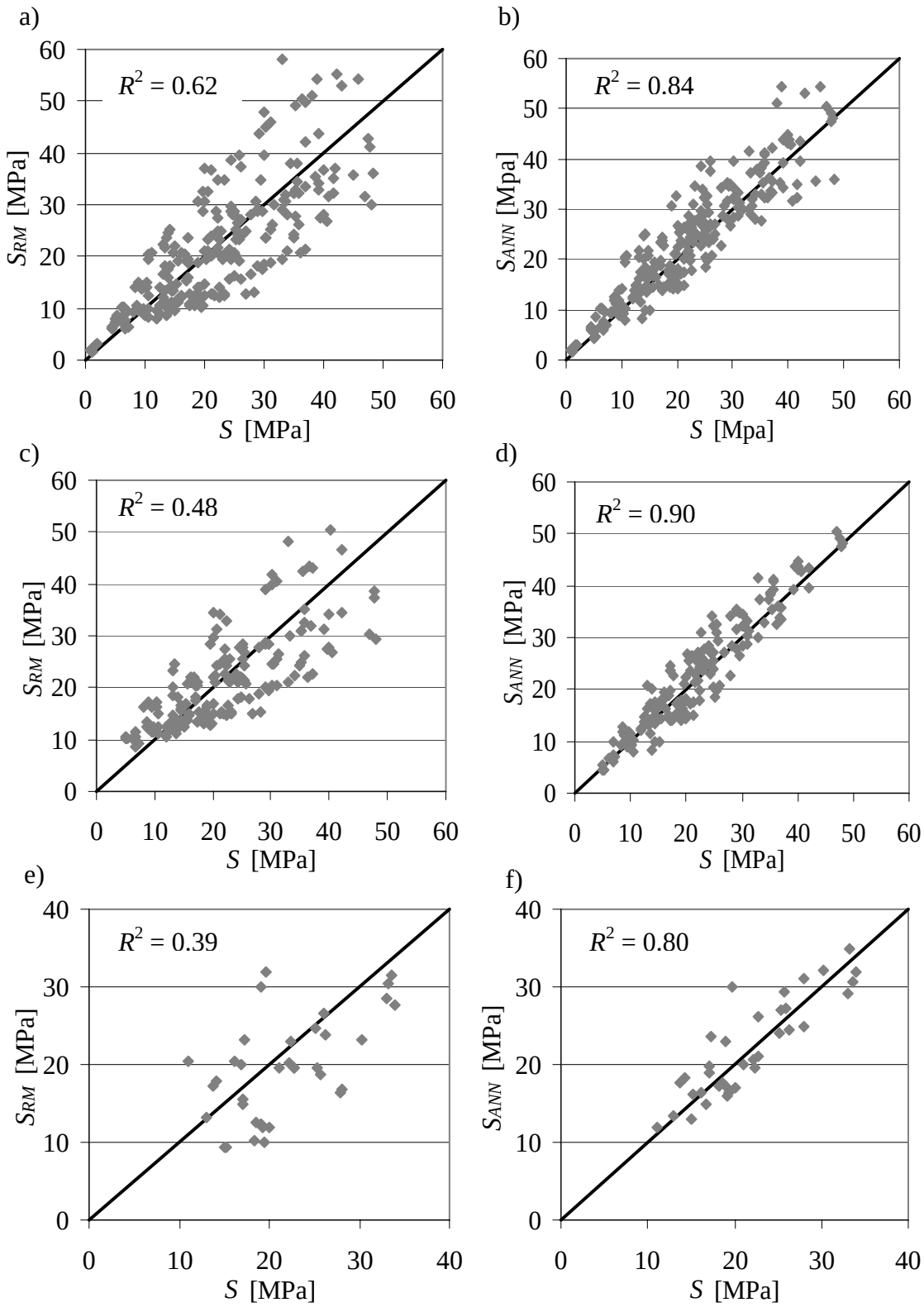

Fig. 9. Efficiency of the proposed numerical model – relationships between
a) S and S_{RM} (model 2), all data,
b) S and S_{ANN}, all data,
c) S and S_{RM} (model 5), part 1,
d) S and S_{ANN}, part 1,
e) S and S_{RM} (model 2), additionally prepared specimens,
f) S and S_{ANN}, additionally prepared specimens.